PAPER • OPEN ACCESS

Evaluation of the functional acceptability of the ITER vacuum vessel

To cite this article: Hokyu Moon *et al* 2023 *Nucl. Fusion* **63** 016003

OPEN ACCESS
IOP Publishing | International Atomic Energy Agency Nuclear Fusion

Nucl. Fusion **63** (2022) 016003 (15pp) https://doi.org/10.1088/1741-4326/aca1d0

Evaluation of the functional acceptability of the ITER vacuum vessel

Hokyu Moon[1,*], Soo-Hyeon Park[1], Hyun-Soo Kim[1] and Beom Seok Kim[2]

[1] ITER Tokamak Engineering Department, Korea Institute of Fusion Energy (KFE), 169-148 Gwahak-ro, Yuseong-gu, Daejeon 34133, Korea, Republic Of
[2] Department of Mechanical and Automotive Engineering, Seoul National University of Science and Technology, 232 Gongneung-ro, Nowon-gu, Seoul 01811, Korea, Republic Of

E-mail: hkmoon@kfe.re.kr

Received 8 July 2022, revised 27 September 2022
Accepted for publication 10 November 2022
Published 25 November 2022

Abstract

The International Thermonuclear Experimental Reactor (ITER) vacuum vessel (VV) is one of the critical components of the ITER tokamak fusion reactor. The first sector of the ITER VV was delivered to ITER Organization in 2020, and it is ready to assemble into the tokamak system. After manufacturing the ITER VV, an evaluation should ensure that the components are designed and manufactured to meet the functional requirements, such as vacuum leak tightness and structural integrity. The factory acceptance test (FAT) is essential for confirming acceptance in engineering and manufacturing. This paper introduces the engineering process and technical method of the FAT, which is applied explicitly to the first-of-a-kind ITER VV. We establish a visual inspection, pre-pumping assessment, pressure test, helium (vacuum) leak test, and final dimensional inspection for the FAT. The visual inspection revealed no blockages in the cooling channels of the double walls. The pre-pumping assessment conducted to check the vacuum level and residual gas condition, concluded that the inside of the VV was flawless and thus met the leak test requirements of 1×10^{-8} Pa m^3 s^{-1}. We confirmed no leakage or deformation through the pressure test under reduced pressure. The helium leak test demonstrated engineering soundness with leak tightness of 6.08×10^{-9} Pa m^3 s^{-1}, which is more stringent than the allowable limit. Furthermore, three-dimensional metrology was utilized to determine the as-built dimensions of the manufactured sector. Due to unavoidable weld deformation and tight tolerances, the as-built result does not perfectly meet the assigned tolerance level. Nevertheless, it can be considered as advanced information for assembly with in-vessel components and other sectors. Based on the conformance and suitability of the suggested FAT for the first ITER VV sector, we will determine the acceptability of the upcoming VV sectors, which will be manufactured and delivered by Korea shortly.

Keywords: tokamak fusion reactor, vacuum vessel, functional acceptance, factory acceptance test, ITER

(Some figures may appear in colour only in the online journal)

* Author to whom any correspondence should be addressed.

1. Introduction

Nuclear fusion power is considered to be a type of next-generation energy due to its plentiful fuels and environmental sustainability with carbon-free heat generation [1–4]. Nuclear fusion induces the fusion of two light atoms of deuterium (D) and tritium (T) and generates an alpha particle of heavier helium and a neutron with 14 MeV of energy [1, 5]. Implementing a highly demanding high-vacuum plasma environment to sustain the fusion reaction on Earth is essential. In particular, as a prerequisite for the generation of fusion power, it is necessary to achieve the burning plasma condition where the fusion reactions are sustained in a well-confined plasma environment. For this purpose, tokamaks have been designed as the most promising way to achieve nuclear fusion [1, 6]. This design consists of a doughnut-shaped toroidal chamber with superconducting magnets that traps the plasma. Plasma confinement is achieved by toroidal and poloidal magnetic fields in the toroidal vacuum vessel (VV). Because the VV is not only a hermetical sealed plasma container but also the first safety barrier, the VV is a critical component of the tokamak to secure the function and relevant safety of its fusion engineering facilities [7].

The International Thermonuclear Experimental Reactor (ITER) is the first nuclear fusion facility to demonstrate the technical feasibility of fusion physics and engineering for the implementation of fusion power generation [8, 9]. The ITER tokamak comprises a VV including blankets and divertors as the plasma-facing components, superconducting magnets (toroidal field system, poloidal field system, central solenoid, corrections coils, magnet feeders, and in-vessel coils), and a cryostat. For the first plasma operation of the ITER, tentatively scheduled for 2025, manufacturing of the principal mechanical components and construction involving their assembly on-site are in progress [9]. The tokamak assembly process started in 2020 as the first tokamak sector to be assembled. The tokamak sector is assembled with the sector of the VV, two toroidal field coils, and a corresponding sector of a thermal shield, and is wholly manufactured with two poloidal field coils [10]. The main functions of the ITER VV is to provide a high-vacuum condition to sustain the stability of fusion plasma, to serve as the first primary confinement barrier against any leakage of radioactive materials, to provide mechanical support for in-vessel components, and to remove the nuclear heating by circulating tons of cooling water [11]. Accounting for the main functions of the VV, the ITER VV is a critical component of the ITER tokamak fusion reactor.

Based on its role as the first safety barrier and mechanical support for plasma-facing components, the ITER VV is classified as a safety-important component and a protection-important component [12]. Specifically, it is classified as category IV pressure equipment under the French Decree on the design and construction of pressure equipment (ESP) and as Nuclear level N2 under the French Order Concerning Nuclear Pressure Equipment because pressurized cooling water (i.e., up to 1.1 MPa in normal operation) is applied during its operation [13, 14]. Moreover, it is categorized as a class-2 welded box structure with supporting and leak-tight components according to RCC-MR 2007, which is the relevant technical guideline pertaining to its design and construction [12–14]. The manufactured ITER VV must comply with the assigned codes, regulations, and ITER requirements, including all manufacturing processes. Therefore, it is essential to evaluate the engineering and manufacturing approval process of VV to ensure functional needs such as vacuum leak tightness and structural integrity after manufacturing is finished. The VV's functional acceptability verification phase consists of several tests, collectively knowns as the factory acceptance test (FAT) [15–18].

This study aims to identify the specific process and technical method of the FAT such that this series of tests will be effective for the first ITER VV considering its functional and safety requirements. Considering the first-of-its-kind sector for the ITER VV, this study lays the groundwork for the feasibility of evaluation methods and the demonstration of results to ensure proper engineering integrity. Systematic approaches have been devised for the first manufactured VV. The functional acceptability assessment was carried out through a visual inspection, a pre-pumping assessment, a pressure test, a helium (vacuum) leak test, and a final dimensional inspection. As the first sector (sector #6) is manufactured and delivered to the ITER Organization [10, 19], the technical details are based on those applied to the first sector of the ITER VV. The evaluation results demonstrate that all ITER VV's FAT elements comply with relevant specifications and technical guidelines, reflecting important functional requirements such as vacuum leak tightness and structural integrity.

2. ITER vacuum vessel and its acceptance for implementation: factory acceptance test (FAT)

The ITER VV has a toroidal double-walled stainless steel (316L(N)-IG) [20] structure divided into nine sectors with an angle of 40° in the circumferential direction. Figure 1 presents the configuration of the comprehensive ITER VV with an image of the first-manufactured sector (sector #6). There is a set of eighteen radial port extensions at the top (upper ports), seventeen ports at the equatorial level (equatorial ports), and nine ports at the lower level (lower ports) for the entry of auxiliary systems to be installed for diagnostics, plasma heating, and vacuum pumping. Furthermore, several mechanical supports and rails exist inside of the vessel wall (i.e., plasma side) to support in-vessel components such as the blanket modules, coils, and blanket manifolds [7, 21].

Regarding the comprehensive features of the ITER VV, the FAT is essential for functional verification of the vacuum leak tightness and structural integrity of the factory-manufactured ITER VV after it is fully manufactured. In particular, the

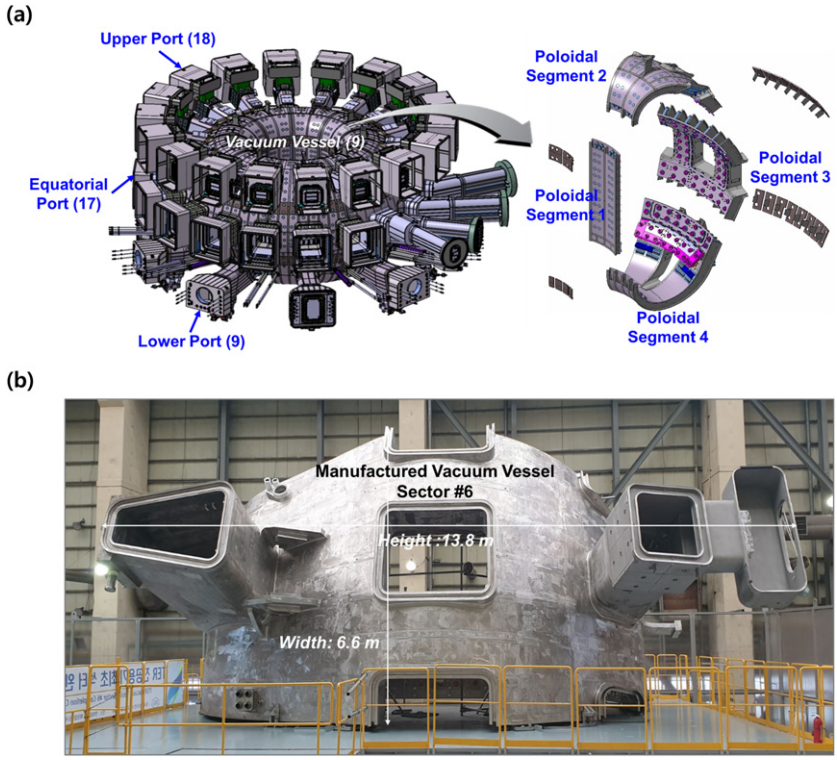

Figure 1. ITER vacuum vessel: (*a*) the ITER vacuum vessel consists of nine vacuum vessels, eighteen upper ports, seventeen equatorial ports, and nine lower ports. Precisely, one vacuum vessel consists of four poloidal segments. (*b*) Manufactured the first sector (sector #06) of the ITER vacuum vessel. It is 13.8 m high (the height of D-shape is 11.4 m) and 6.6 m wide. The total weight of the vacuum vessel sector is 374 tons. The first sector was delivered to the ITER site in August of 2020.

VV components should indicate that engineering safety can be guaranteed through conformance with the RCC-MR 2007 specification. A set of engineering verification procedures was established and conformity was evaluated according to the code and requirements [22]. The Korea Domestic Agency (Korea Institute of Fusion Energy) and the manufacturer Hyundai Heavy Industry Co. have established systematic test procedures.

Figure 2 shows the detailed sequence of the FAT applied to the first sector (sector #6). Among the FAT components, the visual inspection, pre-pumping assessment, and helium leak test are designed to evaluate vacuum-leak-tightness capabilities. In addition, the pressure test and the final dimensional inspection are for the structural integrity assessment. A typical FAT involves a flow test, a pressure test, a baking, a helium leak test, and a final dimensional inspection [23, 24]. However, the FAT for the ITER VV should be reset based on technical feasibility considerations. Because the flow test determines whether the inner channels are clogged, it is more concise and intuitive visually to check during fabrication than to allow the flow into the complex D-shape interior of the VV. Moreover, the pressure test can verify the flow passage inside the D-shaped VV through pressurization. On the other hand, baking is necessary to remove volatiles and molecular species (such as water) that affect the vacuum conditioning and leak test background. Convective baking was planned for the VV sector using a qualified furnace. Despite the fact that the furnace capacity is suitable for VV heat-up and cooling, accurate control of the uniform temperature distribution across the heavy (374 tons) VV given its complex internal geometries within the target schedule will be challenging. Moreover, thermal stress could arise due to a non-uniform temperature distribution if the flow inside the VV is not actively controlled during the baking process [25]. This would give rise to involuntary non-uniform thermal expansions. Thus, baking is replaced with pre-pumping assessment, which can discharge contamination from the surfaces of the internal VV.

2.1. Visual inspection

Figure 3(*a*) presents in-wall shielding (IWS) blocks made of borated stainless steel (SS 304 B7 and SS 304 B4). These are installed in the space between the inner and outer shells (i.e., double walls) of the VV to provide effective neutron shielding. Plated IWS blocks are pre-assembled with an average spacing of 4 mm and then assembled inside the double wall. The gap between the first plate and inner shell is 42 mm, and the gap between the last plate and the outer shell is 78 mm [26]. The coolant circulates through these gaps to cool the VV during the ITER operation. During the FAT, it is also important to ensure that the pumping inside the VV is not clogged for pre-pumping assessment and helium leak testing to evaluate the vacuum leak tightness. Through the visual inspection, we can validate whether there are any flow blockages in the space between the double walls of the VV.

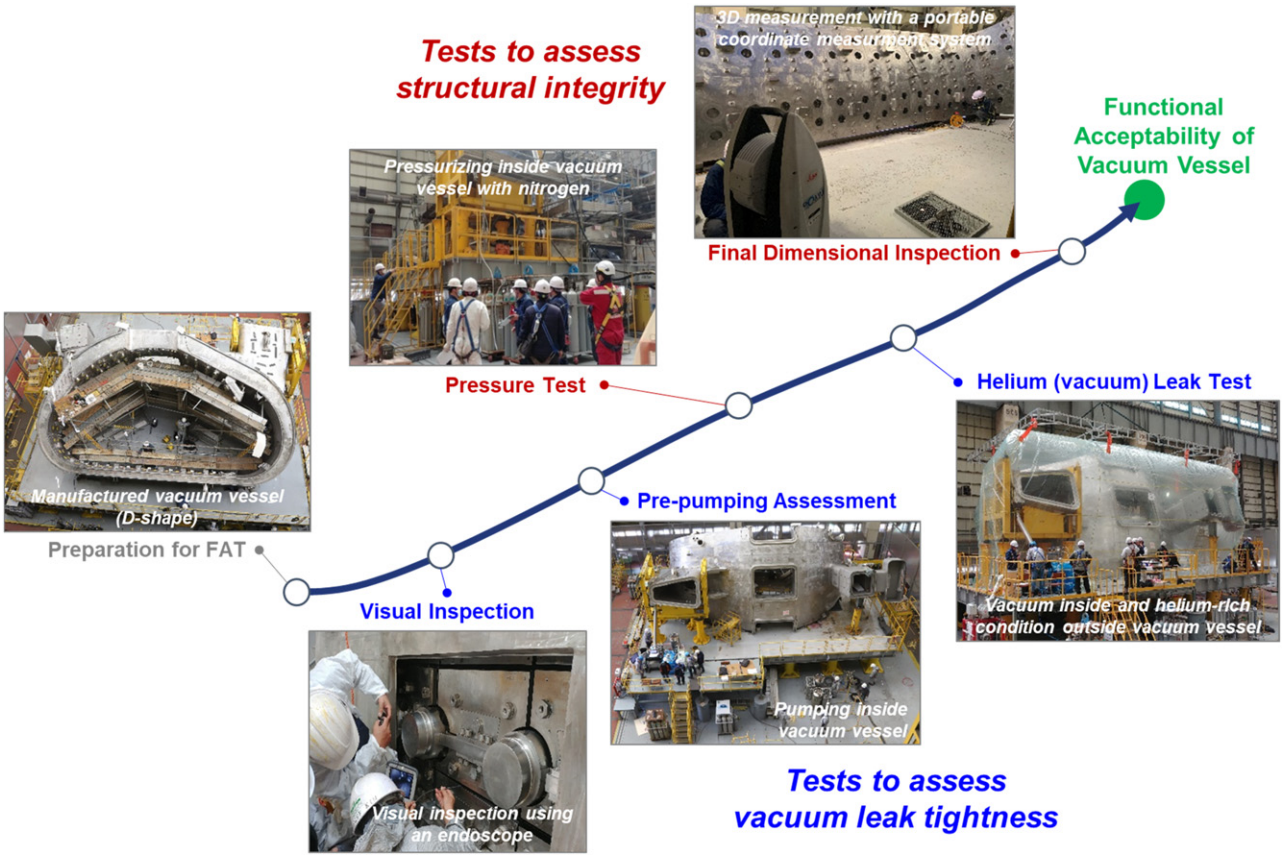

Figure 2. The FAT sequence is applied to the first sector of the ITER vacuum vessel. The FAT process involves a visual inspection, a pre-pumping assessment, a pressure test, a helium (vacuum) leak test, and a final dimensional inspection.

Figure 3(*b*) shows a schematic diagram of the visual inspection. An endoscope (Olympus, IPLEX NX) was applied to each gap in the double-wall to investigate any blockages. The endoscope passes through the channel after checking along each position marking number.

2.2. Pre-pumping assessment

For the VV components, the pre-pumping assessment is essential to reduce contamination on the surfaces and to validate the requirements of the subsequent leak test regarding the vacuum state and leak rate. Figure 4 shows a schematic diagram of the pre-pumping assessment and helium (vacuum) leak test system. The pre-pumping system is connected to the VV lower port stub extension (LPSE). It mainly consists of four individual vacuum pumps: a rotary pump (Duo 125, Pfeiffer), a roots pump (Okta 1000, Pfeiffer), a dry pump (nXL200i, Edwards), and a turbo molecular pump (TMP: Hipace 2300U, Pfeiffer). Specifically, the rotary and roots pumps are connected to the roughing pump (viscous flow), and the TMP and dry pump are connected to the molecular pump flow. Two pressure gauges (P1 and P2: PKR 251, Pfeiffer) are installed and recorded to verify the vacuum condition of the double wall during the pumping process. To check the status of the mass spectrum of the residual gas, a residual gas analyzer (RGA200, Stanford Research Systems) operates when the vacuum level of 5×10^{-2} Pa is reached. The monitoring mass range is from 1 to 100 amu (atomic mass unit).

2.3. Pressure test

A pressure test should be conducted to assess the structural integrity of the VV. The design pressure of the VV and port is 2.60 MPa [11], and the actual load for the pressure test of the full VV is 3.72 MPa according to the RCC-MR 2007 specification (i.e., $P_{\text{test}} = 1.43P_{\text{design,max}}$) [22]. After the 360° entire assembly of the VV at the ITER site, the VV cooling channels will be tested under the calculated pressure condition, 3.72 MPa. As far as the factory pressure test allows, however, for a single sector of the VV, the pressure applied during the assessment is 0.50 MPa under the pneumatic test condition because the actual load by the coolant is 0.50 MPa on the poloidal ribs at the field joint of a single sector during the operation. The pressure should be kept at 0.50 MPa to avoid plastic deformation of the side ribs of the VV sector. The level of 0.50 MPa with the pneumatic condition also prevents the inclusion of water in the space between the double walls that must be evacuated to create a vacuum for the helium leak test. If water is used as the test medium, it should be recognized that crevices may contain water and cause a virtual leak. Regarding these aspects, the pressure test was designated to be performed at 0.50 MPa using nitrogen. Figure 5 shows an image of the actual installation of the pneumatic pressure test system. A

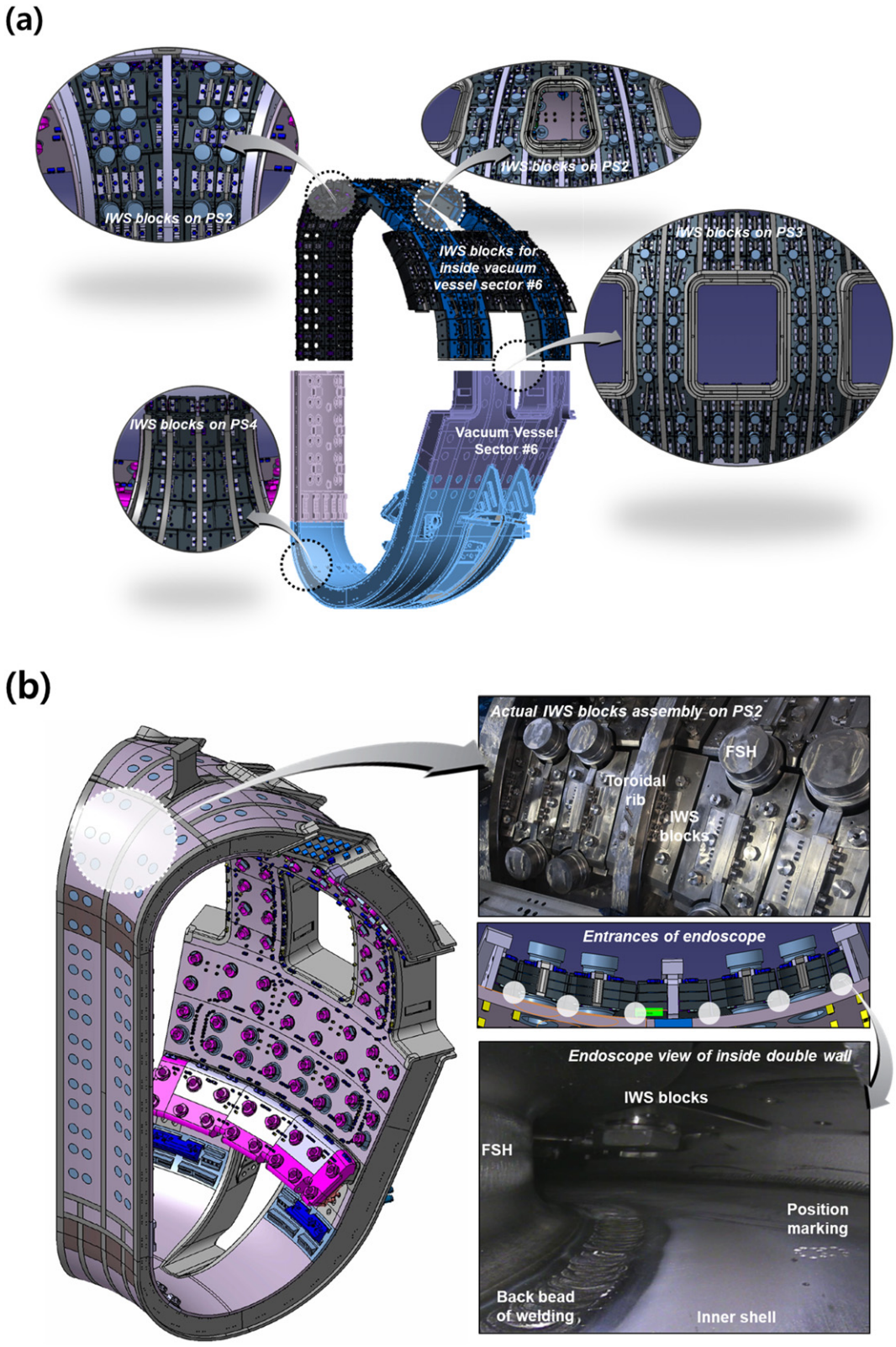

Figure 3. Double inside wall and visual inspection of the vacuum vessel: (*a*) installation of the IWS blocks in vacuum vessel sector #6. (*b*) Schematic diagram of the double-wall interior visual inspection. We examined the cooling channels created by the IWS blocks using an endoscope to check for blockages.

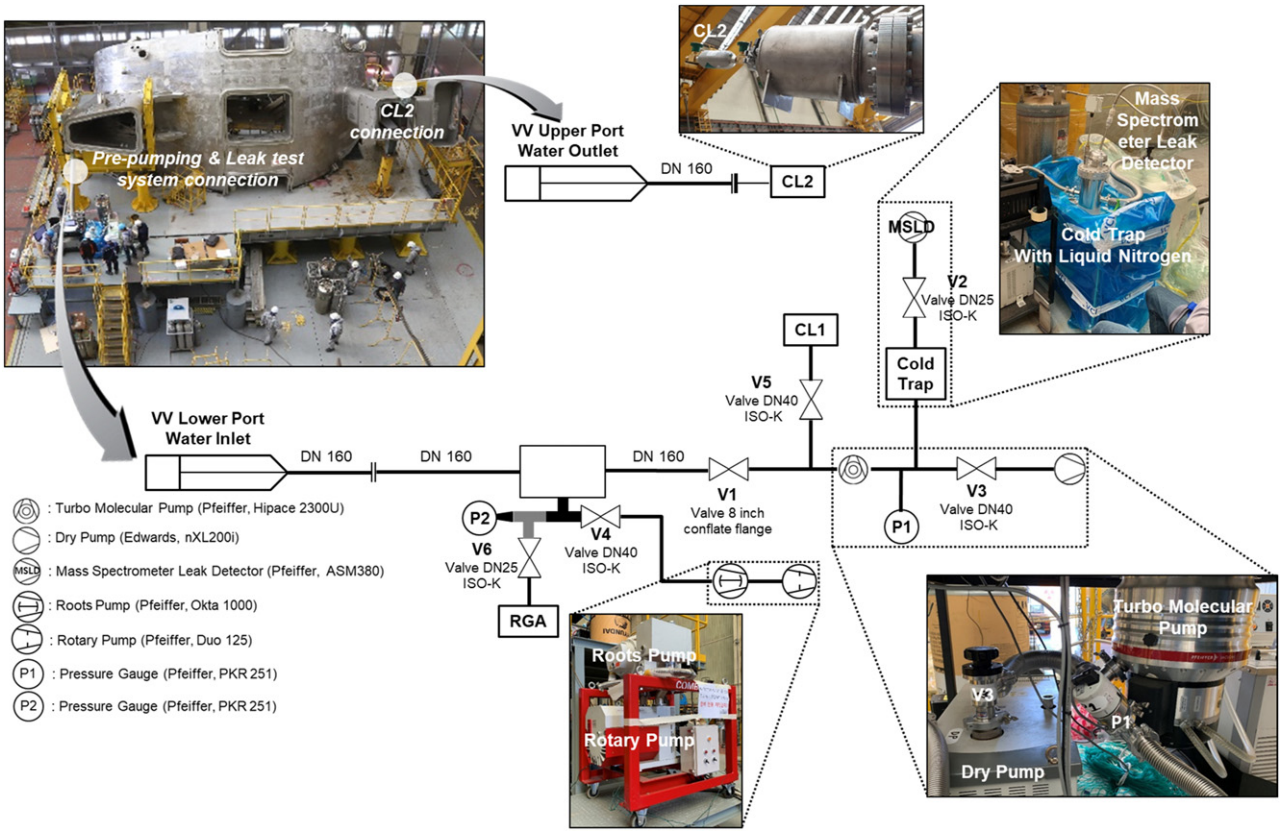

Figure 4. Schematic diagram of the pre-pumping assessment and helium (vacuum) leak test system with pictures of the actual installation. The pre-pumping system consists of a rotary, roots, dry, and turbo molecular pump. Two calibrated leaks (CL1 and CL2), a cold trap, and an MSLD are applied during the helium leak test.

nitrogen gas (5-nine purity) bundle is connected to the water inlet of the VV LPSE and the VV temperature is measured at ten selected points during the test. To check the pressure inside the double wall, two class 0.25 pressure gauges (Dwyer, DPG-100) are installed, one on the LPSE and the other on the upper port stub extension (UPSE). During pressurization and decompression, the values of the two pressure gauges on the LPSE and the UPSE are checked and recorded.

2.4. Helium (vacuum) leak test

A weld approximately 1.5 km long is used to manufacture VV sector #6 for structural supporting and vacuum leak tightness. Regarding the integrity of welding, the leak test is vital in the FAT to ensure the critical functionality of the ITER VV. As a non-destructive test, the helium leak test was employed to determine the leak-tightness requirement of the material and surface of the VV [27–29]. While helium is applied as a tracer, differentiated pressure conditions are controlled inside and outside of the object to allow helium penetration into any conceivable cracks [29]. During the helium leak test, the inside of the VV is evacuated (high vacuum condition to 10^{-1}–10^{-4} Pa) with the pumping system. In contrast, the outside of the VV is maintained at a helium concentration of more than 50% with a designed enclosure at room temperature. The leak rate on the plasma side of the VV must meet the criterion of 1×10^{-7} Pa m^3 s^{-1} even after the torus is assembled [11]. Given that the VV is located between the plasma and the cryostat as the first confinement barrier and mechanical supporting structure, the leak rate should adhere strictly to a rate of less than 1×10^{-8} Pa m^3 s^{-1}.

Figure 4 shows a schematic diagram of the helium leak test system with pictures of the actual installation. The leak test system is connected to the water inlet of the VV LPSE. There are two calibrated leaks in the pre-pumping system, referred to here as CL1 (FV 4700, Pfeiffer, 1.2×10^{-8} Pa m^3 s^{-1}) and CL2 (FV 4310, Pfeiffer, 5.3×10^{-8} Pa m^3 s^{-1}), to provide a known helium mass flow in the system for calibration. In addition, a cold trap and a mass spectrometer leak detector (MSLD: ASM380, Pfeiffer) are included. Primarily, the cold trap is employed for liquid nitrogen to remove water vapor from outgassing, which improves the helium leak detection sensitivity. After checking the leak test system, the MSLD is used to verify the leak rate when the conditions of a vacuum inside the VV and the 50% or more helium-rich conditions outside the VV are met. The sensitivity of the test system must exceed one order of the allowable leak rate [11, 30]. Helium is added to the designed enclosure (nylon vacuum bag, WL 7400, Airtech). The helium concentration is monitored at two points in the enclosure on the opposite side of the helium injection point by katharometers (XP-3140, New Cosmos). The leak rate

Figure 5. The picture of the actual installation of the pneumatic pressure test system. The lower pressure gauge is installed on the LPSE side, and the upper-pressure gauge is installed on the UPSE side. A bundle of five-nine purity nitrogen gas is connected to the LPSE connection.

can be estimated according to the helium leak rate results. It demonstrates the leak tightness of the VV.

2.5. Final dimensional inspection (three-dimensional metrology)

Following the previous series of assessments, three-dimensional inspections were conducted to confirm the as-built condition of VV sector #6. The inspections were conducted in the laying position of the VV sector (figure 1) as agreed with the ITER Organization. The measurements were manually done made by moving a retro-reflector (discrete or continuously) across all surfaces of the VV, with a laser tracker continuously tracking the laser reflected from the retro-reflector [31]. The feedback signal is recorded in the metrology software along with the CAD model in the specified coordinate system. It is challenging to measure the actual characteristics of such a large VV (height 11.4 m) under measurement uncertainty of several hundred micrometers. Specifically, the measurement system as devised here secures the movement of the reflector within 60 μm, instrument drift within 150 μm, object temperature deviation within ± 1 °C, and the estimated cumulative uncertainty within 200 μm during the measurement. Figure 6 shows the three-dimensional measurement scheme and strategy for the final dimensional inspection. A portable coordinate measuring system with a laser tracker (AT 960, Leica Absolute Tracker), a retro-reflector, and portable metrology software (SpatialAnalyzer, HEXAGON, and PolyWorks, InnovMetric, respectively) are employed for the measurement [19, 32–34]. Because multiple measurements are undertaken, the application of a fiducial post (mounting of the target nest and retro-reflector) is required as a physical reference (figure 6(*a*)). Moreover, measurements are impossible with only a single setting of the measuring instrument for the VV sector. They can be done by applying several settings, though this affects the measurement uncertainty [31]. After measurement with the SpatialAnalyzer, an advanced bundling technique (i.e., unified spatial metrology network) is applied to avoid the accumulation of measurement uncertainty (2σ) in the three-dimensional measurement results. The as-built result is then fitted to the nominal CAD model using what is termed the minimizing relationship method (i.e., move objects by minimizing relationships), taking the global datum system into account. Figure 6(*b*) shows the three-dimensional measurement strategy for the final dimensional inspection. All tolerances and datum systems given for the VV must initially be checked [35]. Manufacturing tolerances are primarily based on the capabilities of the VV and are subject to geometric dimensioning and tolerance (GD & T) standards according to the assigned values [36, 37]. When performing as-built 3D measurement of the VV, care must be taken to minimize measurement uncertainty, mainly due to instrumental drift and temperature changes. Finally, a GD & T analysis was conducted using the 3D construction results.

3. Results and discussion

3.1. Vacuum leak tightness upon visual inspection, pre-pumping assessment, and helium leak test

The visual inspection, pre-pumping assessment, and helium leak test evaluate the vacuum-leak-tightness capabilities of the VV. All visual inspections by third-party inspectors with expertise confirmed that the cooling channels in the double wall were not blocked. This indicates that the pumping inside

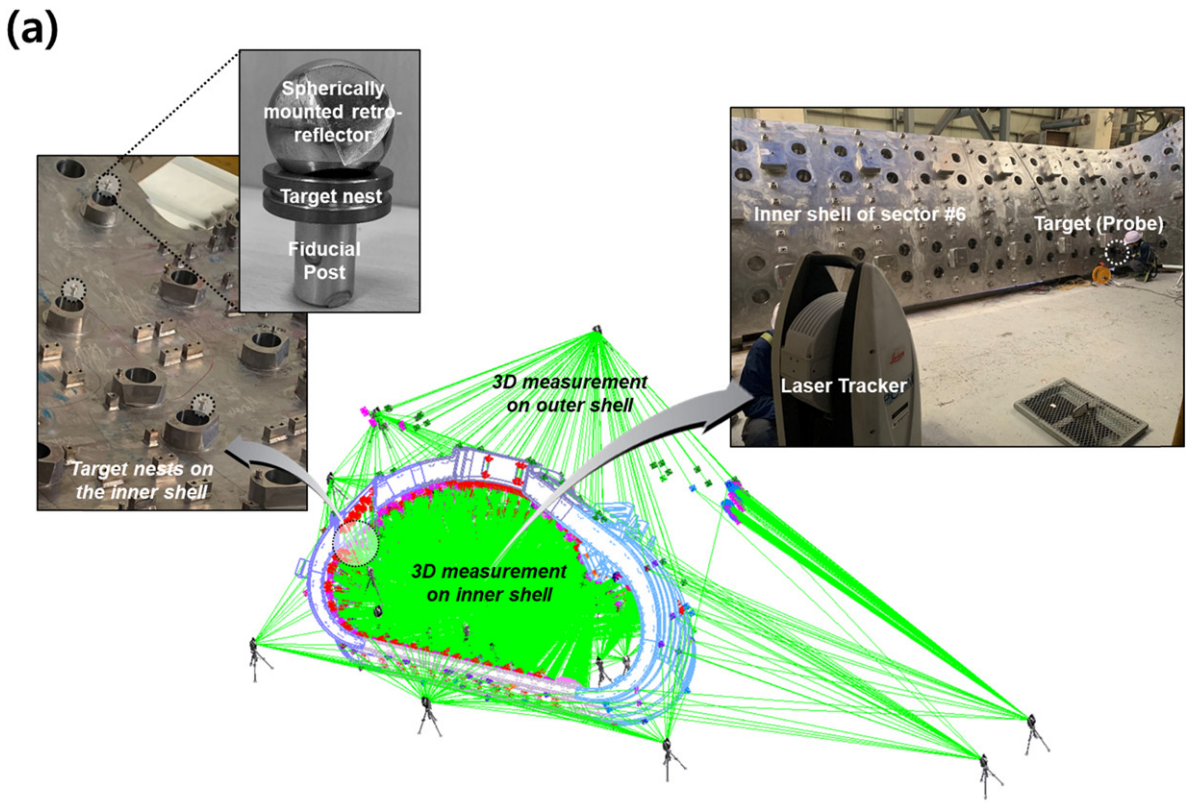

Figure 6. Three-dimensional measurement scheme and final dimensional inspection strategy: (*a*) actual 3D measurements using a laser tracker and fiducial posts as the final dimensional inspection of sector #6. (*b*) Three-dimensional measurement strategy for the final dimensional inspection.

the VV is not clogged for the pre-pumping assessment and helium leak test. Figure 7 shows the pre-pumping assessment results according to a sequential pump operation. After operating the rotary pump for 12 h, the pressure inside the VV reached a plateau of 900 Pa. After turning on the roots pump, the pressure went to approximately 20 Pa within 3.5 h. The free volume inside the VV is about 20 m^3, but the surface area of the interspace of the VV is 1509 m^2 due to the IWS blocks.

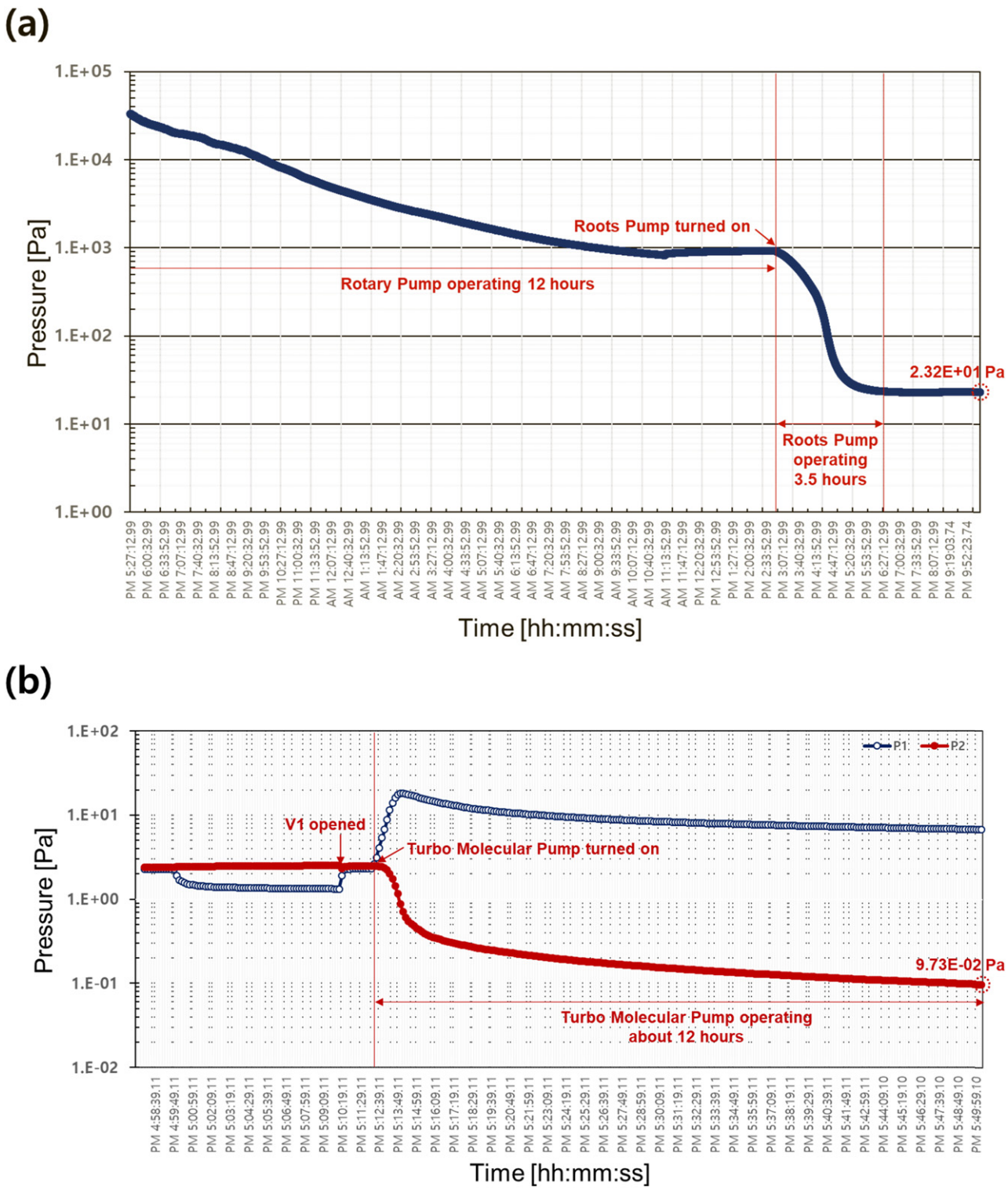

Figure 7. Pressure variation during the pre-pumping assessment: (*a*) time trace of the pressure variation during rough pumping (operation of the rotary pump and roots pump), and (*b*) time trace of the vacuum level during the operation of the turbo molecular pump and dry pump (P2 is the vacuum level inside the vacuum vessel).

The rough pumping took longer than expected owing to the complex geometry and consequent large surface area of the IWS blocks. After rough pumping, the dry pump and the TMP were started while checking the vacuum level. After operating the TMP for about 12 h, the vacuum level reached 10^{-1} Pa (9.73×10^{-2} Pa), as shown in figure 7(*b*). It is confirmed that the VV can hold the necessary vacuum condition on the inside double wall to check the vacuum-leak-tightness via the helium leak test.

Figure 8 shows the results of the analysis of the mass spectrum of the residual gas during the pre-pumping assessment. The highest partial pressure appears at 18 amu, indicating

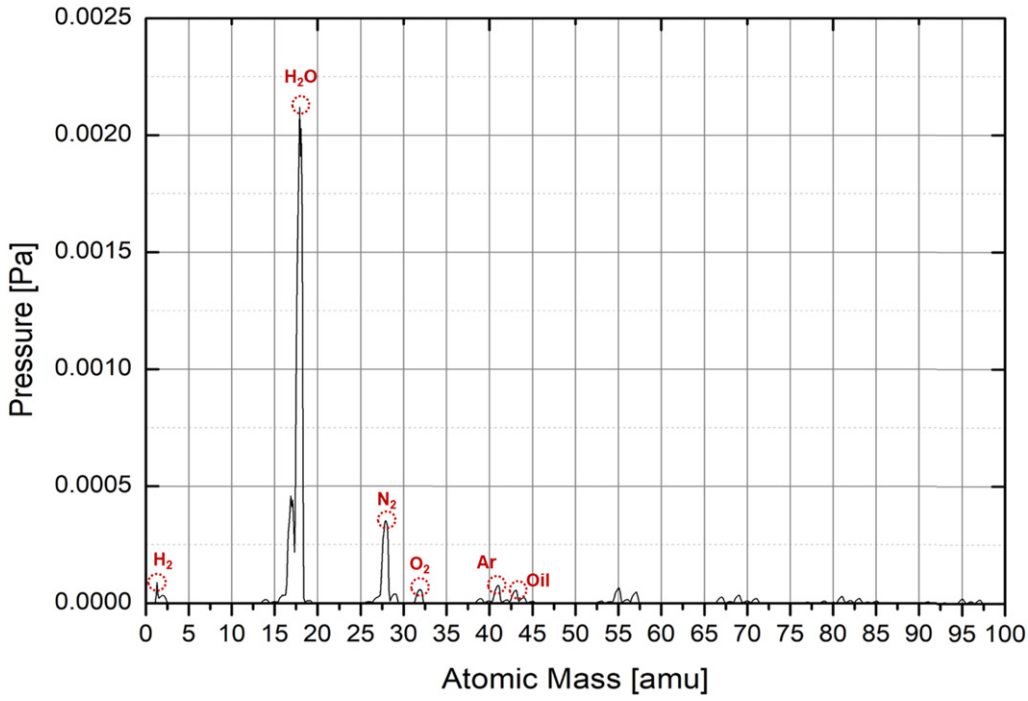

Figure 8. Analyzed mass spectrum of the residual gas during pre-pumping; H_2 (2 amu), H_2O (18 amu), N_2 (28 amu), O_2 (32 amu), Ar (41 amu), and oil (43 amu) appear.

that the main component of the residual gas is water vapor. Because the VV is constantly exposed to the atmosphere as it is manufactured, water vapor and air can easily be absorbed into the surface [30, 38]. The composition of air, which is H_2 (2 amu), N_2 (28 amu), and O_2 (32 amu), constitutes the second-largest amount of residual gas (mainly N_2), with argon (41 amu) being third. Argon is utilized as a purging gas for tungsten inert gas (TIG) welding of the entire VV. Finally, oil (43 amu) comes out, which can be mechanical pump oil by the rotary pump or processing oil when machining the segment before the D-shaped assembly [19]. The mass spectrum of residual gas can confirm that the inside of the VV is clean enough to meet the leak test requirement without baking.

Figure 9 shows the helium leak test results under the vacuum condition and the helium leak rate inside the VV. We locally sprayed helium to check for any leaks in the vacuum fitting connections in the leak test systems and then confirmed that there were no leakages by checking for any changes in the helium leak rate. While helium filled the enclosure, the vacuum level inside the VV (P2) was monitored, showing a stable value of 2.2×10^{-3} Pa, as shown in figure 9(*a*). After reaching a 50% helium concentration in the enclosure, the leak rate was calculated using the formula set in code EN13185 [30] with the selected helium leak rate. The calculated leak rate V_{Leak} is determined as follows:

$$V_{\mathrm{Leak}} = \frac{\left(S_{\mathrm{Leak}} - S_{\mathrm{Leak-Background}}\right)}{\left(S_{\mathrm{Ref}} - S_{\mathrm{Ref-Background}}\right)} \times V_{\mathrm{Ref}} \times \frac{100}{C_{\mathrm{He}}}, \quad (1)$$

where S_{Leak} is the helium background (the helium leak rate inside the VV as provided by the MSLD) that appears at the end of the hold time after the helium concentration reaches 50% outside the VV, $S_{\mathrm{Leak\text{-}Background}}$ is the stable reading of the helium background when the 50% helium concentration is achieved outside of the VV, S_{Ref} is the helium background that appears at the end of the response time after opening the calibrated leak, $S_{\mathrm{Ref\text{-}Background}}$ is the stable reading of the helium background before opening the calibrated leak, V_{Ref} is the nominal value of the calibrated leak, and C_{He} is the helium concentration outside the VV. Figure 9(*b*) shows the helium leak rate variation while maintaining a helium-rich condition exceeding 50% outside of the VV and checking the response time. The response time is the time it takes for the helium to reach the leak detector if it enters the system through any leak. It should be checked before establishing a helium-rich condition outside of the object. However, if helium flows into the VV, it will become trapped inside the VV and a virtual leak may occur. Therefore, it was decided to check the response time after sufficiently maintaining a helium-rich condition. The response time can be considered over 90% of the helium signal arising from a leak (in this case, CL2 opened) to be detected by the MSLD, and it appeared for 16 min (figure 9(*b*)). The holding time must be at least three times the response time according to the RCC-MR 2007 specification. The holding time must be at least 48 min, and the actual hold time was 50 min, which is sufficient. We applied the selected helium leak rate (S_{Leak}, $S_{\mathrm{Leak\text{-}Background}}$, S_{Ref}, and $S_{\mathrm{Ref\text{-}Background}}$) to equation (1) to calculate the leak rate (V_{Leak}), as shown in table 1. The calculated leak rate (V_{Leak}) is 6.08×10^{-9} Pa m^3 s^{-1}, more stringent than the acceptance criteria of 1×10^{-8} Pa m^3 s^{-1}. Vacuum leak tightness is thus verified through the visual inspection, pre-pumping assessment, and helium leak test results.

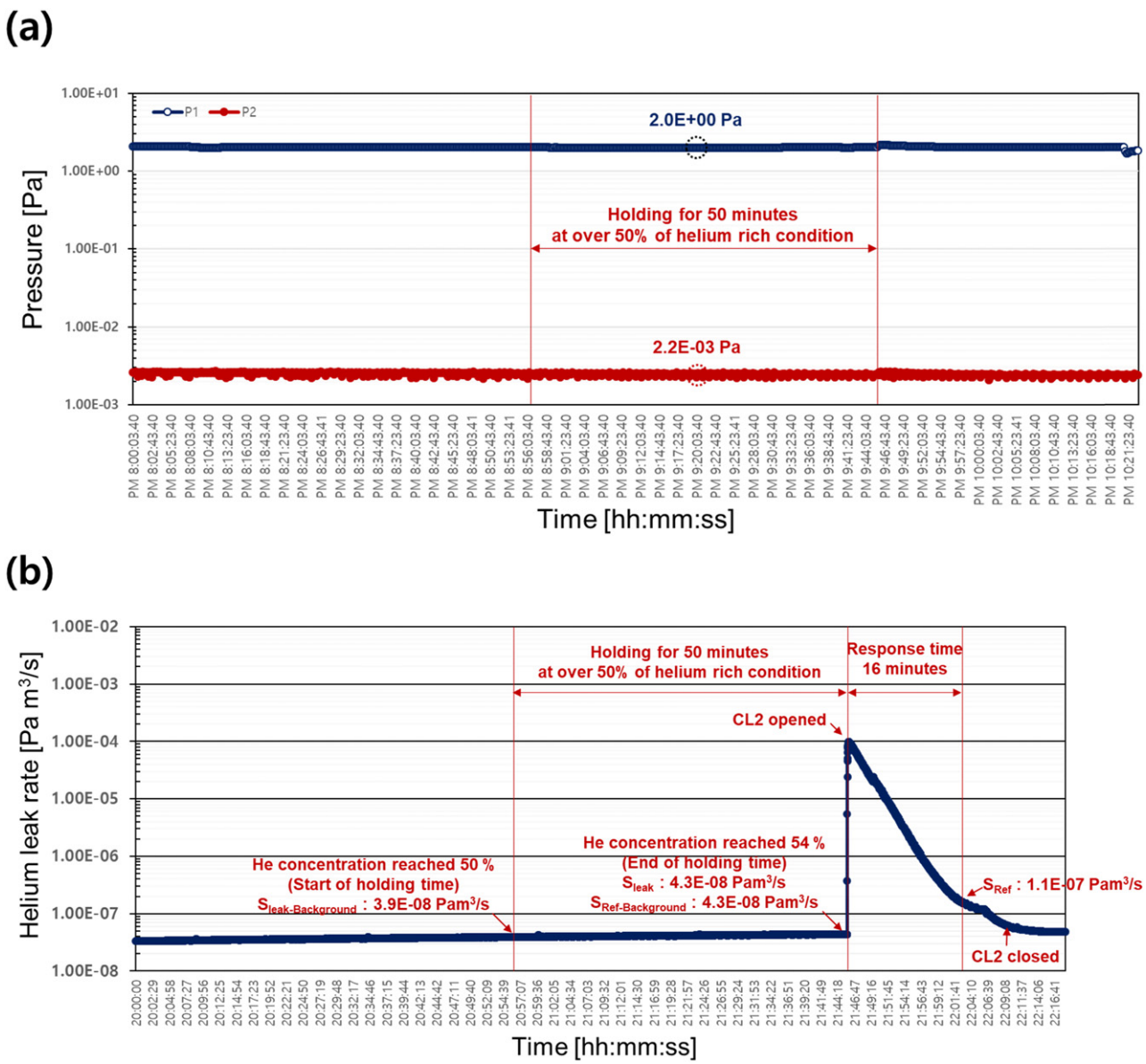

Figure 9. Pressure and helium leak rate variation while maintaining a 50% helium enrichment condition outside the vacuum vessel and checking the response time: (*a*) time trace of the pressure variation (P2 is the vacuum level inside the vacuum vessel), and (*b*) time trace of the helium leak rate of the inside vacuum vessel.

Table 1. Variables and values for leak rate calculation.

Variable	Value
V_{Ref} (Pa m^3 s^{-1})	5.30×10^{-8}
S_{Ref} (Pa m^3 s^{-1})	1.10×10^{-7}
$S_{Ref\text{-}Background}$ (Pa m^3 s^{-1})	4.30×10^{-8}
S_{Leak} (Pa m^3 s^{-1})	4.30×10^{-8}
$S_{Leak\text{-}Background}$ (Pa m^3 s^{-1})	3.90×10^{-8}
C_{He} (%)	5.20×10^{1} (average value)
V_{Leak} (Pa m^3 s^{-1})	6.08×10^{-9}

3.2. Structural integrity upon a pressure test and final dimensional inspection

The assessment results from the pressure test and the final dimensional inspection can demonstrate the structural integrity of the VV. After the pre-pumping assessment, a pneumatic pressure test was conducted using nitrogen. The pressure was maintained in the space between the inner and outer shells, and the average temperature of the VV was 15 °C. There are three holing steps for pressurization up to 5 bar for the test, and there is one step for depressurization at 4 bar. Figure 10 shows the actual pressure steps and results. Each holing step should last for at least 30 min to check the pressure drop and to perform the visual inspections. At the peak condition of 5 bar, bubble tests with a visual inspection were performed randomly to verify leaks and to check for any visible deformation. We confirmed no deformation after relieving the pressure through the final visual inspection. In addition, pressurized nitrogen before the leak test can improve the cleanliness inside the VV and IWS blocks when flushing the nitrogen.

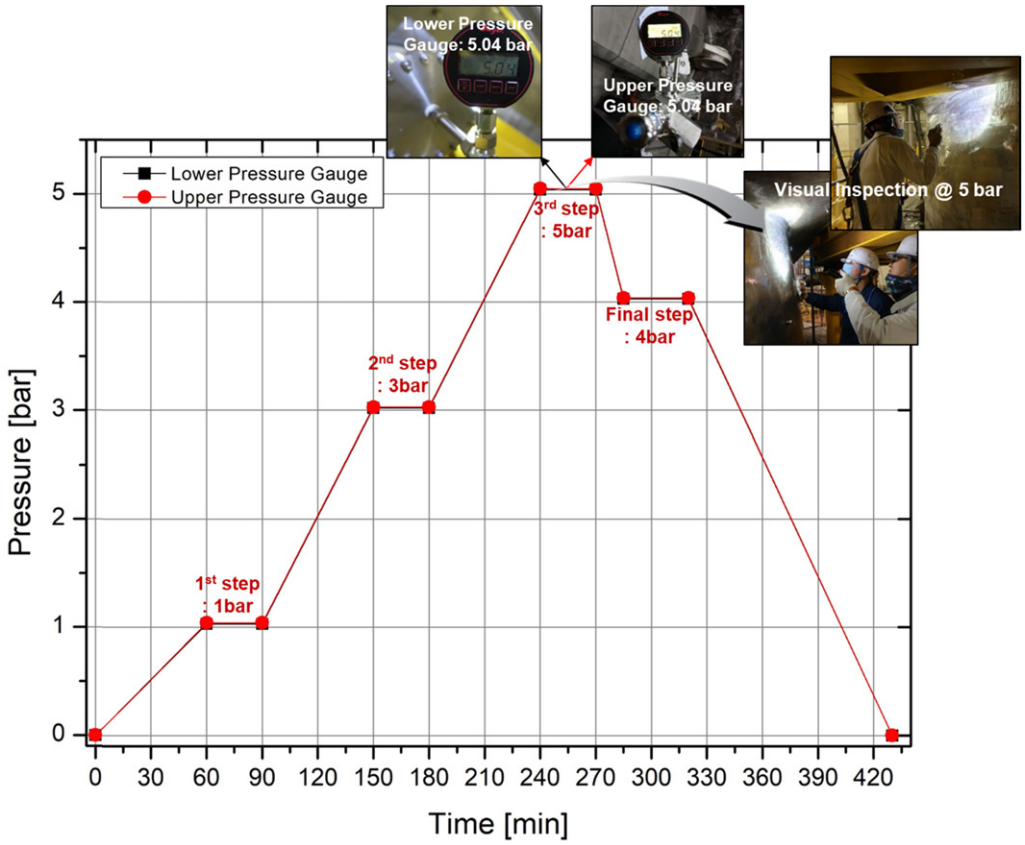

Figure 10. Pneumatic pressure test steps for the applied pressure and hold time. At 5 bar, bubble tests with a visual inspection were conducted randomly to check for leaks and any visible deformation.

Figure 11 shows the as-built result of the inner shell on VV sector #6. The inner shell is the first shield plate during operation, and it has many interfaces with in-vessel components such that the inner shell results are mainly introduced when presenting the as-built results. Before analyzing this result, the as-built results were fitted to a nominal CAD model using the least square method, minimizing the relationship method in the SpatialAnalyzer [19, 33, 39] considering the datum system. The given tolerance for the inner shell surfaces is a profile of 20 mm [35]. Including the shell tolerances, the tolerances of the ITER machine were derived using a statistical variation analysis based on Monte Carlo simulations considering the manufacturing, assembly, and tokamak functional and interface requirements [35, 36]. The satisfaction rates for the tolerance were 99.98% for PS1, 95.87% for PS2, 95.48% for PS3, and 96.48% for PS4. PS2, PS3, and PS4 are out of the local area's tolerance of up to 10 mm in the radial direction. Despite the fact that applying a specially designed jig and fixture while also controlled the welding heat input and speed, welding deformation was unavoidable due to the absolute quantity of the welding [33, 40–42]. The final dimensional inspection confirmed the as-built condition of manufactured VV sector #6. Due to unavoidable weld deformation and tight tolerances, the as-built result does not perfectly meet the assigned tolerance level. Deviations from the tolerances found in the final dimensional inspection were summarized in a non-conformity report (NCR) and issued for official control in ITER Organization [42]. Even if not all as-built results meet the given tolerances, they provide good information with regard to preparing sequential components.

3.3. Verified FAT for the following VV sectors

The first VV sector's FAT results prove that the identified process and method are sufficient to evaluate the functional acceptability of both vacuum leak tightness and structural integrity. All identified processes and methods were performed in the laying position of the VV sector. Significantly, vacuum leak tightness was re-confirmed through the site acceptance leak test by ITER after delivery to ITER [10]. Therefore, we applied similar approaches and techniques for the following VV sectors, i.e., sector #7 and sector #8 (sector #1, which is the last sector of Korea's responsibility, will also be applied). Technically, we demonstrated that vacuum-leak tightness could be achieved only with sufficient pumping inside the VV without baking. For the following VV sectors, a visual inspection, pressure test, helium leak test, and final dimensional inspection are used to evaluate the functional acceptability.

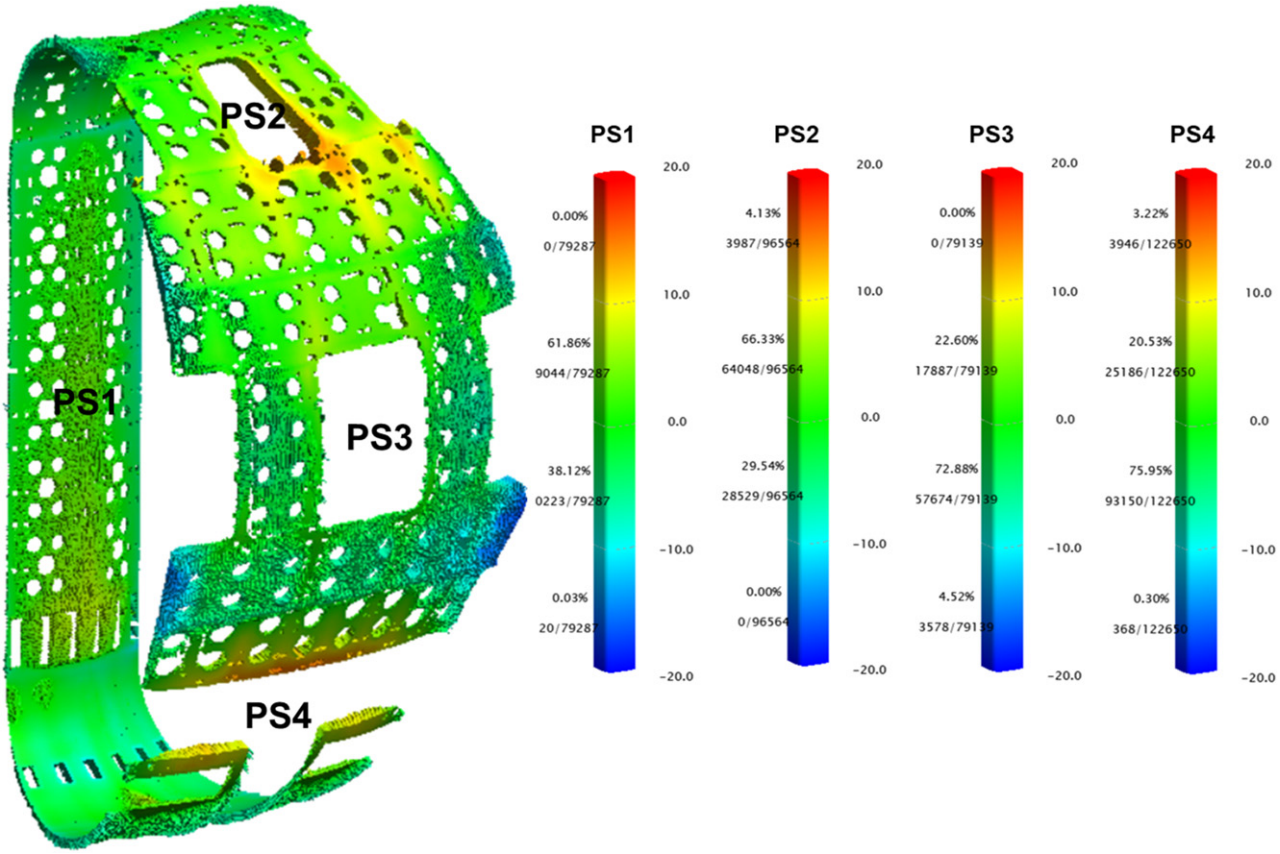

Figure 11. As-built profile of the inner shell of vacuum vessel sector #06. This is the scan result, and the numbers of measuring points are as follows: PS1: 79287, PS2: 96564, PS3: 79139, and PS4: 122650. The tolerance assigned to the inner shell is a profile of 20 mm, and the satisfaction rates with the tolerances are 99.98% (61.86% + 38.12%) for PS1, 95.87% (66.33% + 29.54%) for PS2, 95.48% (22.60% + 72.88%) for PS3, and 96.48% (20.53% + 75.95) for PS4.

4. Conclusions

This study aims to introduce the specific process and technical method of the FAT applied to the first sector (sector #6) of the ITER VV. After the completion of manufacturing, these components should be evaluated to ensure they are designed and manufactured to meet certain functional requirements, such as vacuum leak tightness and structural integrity. The FAT as devised is an essential process to assess the functional qualification of the ITER VV manufactured in the shop. It is categorized into two principal evaluations: a leak tightness function and structural integrity. The FAT assessment of the ITER VV demonstrated the necessary functional requirements with the following results:

(a) We have devised the process and facilities for the FAT, which is proper for the ITER VV. Justifying the technical feasibility, the applied FAT covers a visual inspection, pre-pumping assessment, pressure test, helium (vacuum) leak test, and final dimensional inspection. The visual inspection, pre-pumping assessment, and helium leak test assess the vacuum leak tightness. The pressure test and the final dimensional inspection are to ensure the structural integrity.

(b) The vacuum leak tightness of the ITER VV was evaluated. The visual inspection revealed no blockages in the cooling channels between the double walls. We also validated that the inside of the VV is clean enough to meet the leak test requirement without baking through the vacuum level and the mass spectrum of the residual gas. The first sector of the VV can guarantee leak tightness to 6.08×10^{-9} Pa m^3 s^{-1}, which is more stringent than the acceptance criteria.

(c) The structural integrity of the ITER VV was confirmed by an inspection of any possible leakages and/or deformation through a pressure test. The as-built dimensions for the manufacturing sector were implemented as a principal determinant of the structural integrity. Due to unavoidable weld deformation and tight tolerances, the as-built result does not perfectly meet the assigned tolerance level. Deviations from the tolerances found in the final dimensional inspection were summarized in an NCR and issued for official control in ITER Organization. Nevertheless, the results contribute to the preparation of sequential components for tokamak assembly and provide lessons learned that can be applied when manufacturing subsequent VV sectors.

(d) The first VV sector's FAT results prove that the identified process and method are sufficient to evaluate the functional acceptability. We applied the proven FAT to Korea's remaining VV sectors.

Acknowledgments

This work was supported by the National R & D Program through the National Research Foundation of Korea (NRF), funded by the Ministry of Science & ICT (No. 2007-2006979, Development and Procurement of ITER Vacuum Vessel).

ORCID iDs

Hokyu Moon https://orcid.org/0000-0001-5493-6646
Beom Seok Kim https://orcid.org/0000-0002-1182-1141

References

[1] Entler S., Horacek J., Dlouhy T. and Dostal V. 2018 Approximation of the economy of fusion energy *Energy* **152** 489–97
[2] Rossi R., Gaudio P., Martellucci L. and Malizia A. 2021 Numerical simulations of radioactive dust particle releases during a loss of vacuum accident in a nuclear fusion reactor *Fusion Eng. Des.* **163** 112161
[3] Syblík J., Entler S., Veselý L., Štěpánek J. and Dostál V. 2022 Fusion DEMO sCO_2 layout design with battery farm *Energy* **249** 123730
[4] Kim B.S., Hong S.H. and Kim K. 2022 Preliminary assessment of the safety factors in K-DEMO for fusion compatible regulatory framework *Sci. Rep.* **12** 1–12
[5] Varandas C. 2008 EURATOM strategy towards fusion energy *Energy Convers. Manag.* **49** 1803–9
[6] Juarez R., Pedroche G., Loughlin M.J., Pampin R., Martinez P., De Pietri M. and Sanz J. 2021 A full and heterogeneous model of the ITER tokamak for comprehensive nuclear analyses *Nat. Energy* **6** 1–8
[7] Ioki K., Choi C.H., Daly E., Dani S., Davis J., Giraud B. and Wu S. 2012 ITER vacuum vessel design and construction *Fusion Eng. Des.* **87** 828–35
[8] Zhang T. *et al* 2021 Review on space energy *Appl. Energy* **292** 116896
[9] Bigot B. 2019 ITER construction and manufacturing progress toward first plasma *Fusion Eng. Des.* **146** 124–9
[10] Bigot B. 2022 Preparation for assembly and commissioning of ITER *Nucl. Fusion* **62** 042001
[11] Giraud B. 2009 DDD 1.5 vacuum vessel IDM 22FPWQ, v3.2
[12] Kim H.S. *et al* 2015 Manufacturing design of the ITER vacuum vessel lower port in Korea *Fusion Eng. Des.* **101** 175–9
[13] Martinez J.M. *et al* 2016 ITER vacuum vessel structural analysis completion during manufacturing phase *Fusion Eng. Des.* **109–111** 688–92
[14] Barabash V. *et al* 2010 Codes and standards and regulation issues for design and construction of the ITER mechanical components *Fusion Eng. Des.* **85** 1290–5
[15] Banetta S. *et al* 2015 Manufacturing and testing of a ITER first wall semi-prototype for EUDA pre-qualification *Fusion Eng. Des.* **98–99** 1211–5
[16] Moon H., Park C., Kim G.H., Kim H.S., Kim Y.G., Hong K.H., Kim W.H., Sa J.-W. and Chung W.-H. 2018 Detail procedure of pressure and baking test for ITER vacuum vessel lower port stub extension *Fusion Eng. Des.* **136** 1514–7
[17] Guerrini L., Riccardi B., Andrade J., Escourbiac F., Felip M., Ferrand L. and Lorenzetto P. 2021 Fabrication of ITER divertor Cassette body prototypes *Fusion Eng. Des.* **162** 112054
[18] Valente M. *et al* 2021 Manufacturing, on-site installation and acceptance test activities of the MITICA vacuum vessel *Fusion Eng. Des.* **169** 112473
[19] Moon H., Kim H.S., Lee J., Lim K. and Choi J. 2021 Strategy for D-shape assembly of ITER vacuum vessel sector #06 as applying 3D metrology *Fusion Eng. Des.* **169** 112476
[20] Barabash V. *et al* 2007 Materials challenges for ITER—current status and future activities *J. Nucl. Mater.* **367–370** 21–32
[21] Choi C.H., Sborchia C., Ioki K., Giraud B., Utin Y., Sa J.W. and Savrukhin P. 2014 Status of the ITER vacuum vessel construction *Fusion Eng. Des.* **89** 1859–63
[22] AFCEN R.M. 2007 Design and construction rules for mechanical components of nuclear installations
[23] Moon H. *et al* 2019 Convective baking test of the ITER lower port for factory acceptance *Fusion Eng. Des.* **146** 598–602
[24] Moon H., Kim H.S., Kim Y.G., Park C., Kang S.G. and Lee J. 2020 Hydrostatic pressure test of the ITER lower port stub extension for factory acceptance *Fusion Eng. Des.* **160** 111929
[25] Moon H., Kim K.M., Park J.S., Kim B.S. and Cho H.H. 2015 Thermo-mechanical analysis of an internal cooling system with various configurations of a combustion liner after shell *Heat Mass Transfer* **51** 1779–90
[26] Richard L.S., Bonifetto R., Zanino R., Corpino S., Obiols-Rabasa G., Izquierdo J. and Utin Y. 2013 CFD analysis of a regular sector of the ITER vacuum vessel: I. Flow distribution and pressure drop *Fusion Eng. Des.* **88** 3272–9
[27] Govindaraju M., Ananthakrishnan R., Khan N., Magar M., Nayakwade C., Bardepur R. and Balasubramanian K. 2017 Design of special adapters and furnace for hot helium leak testing of plasma physics components *Mater. Today* **4** 3652–8
[28] Hirai T. *et al* 2017 Examinations for leak tightness of actively cooled components in ITER and fusion devices *Phys. Scr.* **T170** 014045
[29] Calcatelli A., Bergoglio M. and Mari D. 2007 Leak detection, calibrations and reference flows: practical example *Vacuum* **81** 1538–44
[30] Leng Z., Chen J., Wang K., Wang P. and Xu M. 2020 Hot helium leak test of ITER blanket shield block *Fusion Eng. Des.* **153** 111498
[31] Sahu R.K. 2021 A review on application of laser tracker in precision positioning metrology of particle accelerators *Precis. Eng.* **71** 232–49
[32] Shibama Y. *et al* 2017 Assembly technologies of the vacuum vessel on JT-60SA with high accuracy *Fusion Eng. Des.* **125** 1–8
[33] Gu Y. *et al* 2020 Study on the dimensional metrology and alignment method for the 1/32 CFETR VV mock-up *Fusion Eng. Des.* **155** 111556
[34] Liu Z. *et al* 2020 R & D achievements for vacuum vessel towards CFETR construction *Nucl. Fusion* **60** 126024
[35] Fuentes F.J., Trouvé V., Cordier J.J. and Reich J. 2016 Methodology for dimensional variation analysis of ITER integrated systems *Fusion Eng. Des.* **109–111** 315–20
[36] Fuentes F.J., Trouvé V., Blessing E., Cordier J.J. and Reich J. 2013 Status of ITER dimensional tolerance studies *Fusion Eng. Des.* **88** 597–601
[37] Standard A.S.M.E. 1994 *Dimensioning and Tolerancing, ASME Y14. 5M-1994* (New York: American Society of Mechanical Engineers)
[38] Baldzuhn J., Reimer H., Biedermann , Grote D., Hathiramani P., Kornejew O., Rademann D. and Volzke O. 2015 Vacuum leak

search on the Wendelstein 7-X cryostat vessel *Vacuum* **115** 89–100
[39] KINEMATICS N.R. 2013 *Spatial Analyzer User Manual* (Williamsburg)
[40] Matsunaga G. *et al* 2022 Achievement of precise assembly of the JT-60SA superconducting tokamak *Fusion Eng. Des.* **174** 112961
[41] Kamada Y., DiPietro E., Hanada M., Barabaschi P., Ide S., Davis S. and Sozzi C. 2021 Completion of JT-60SA construction and contribution to ITER *Nucl. Fusion* **62** 042002
[42] Hyunsoo K.I.M., Moon H., Park C., Yungjin J.U.N.G., Minsu H.A., Soohyeon P.A.R.K. and Jungjin L.E.E. 2022 Manufacturing completion of the first ITER vacuum vessel sector *Nucl. Fusion* **62** 076044